

High pressure studies on superconducting materials

S Natarajan, T S Sampath Kumar*, S Arumugam, T S Subba Raman,
M D Shaji Kumar and N Victor Jaya

Department of Physics, Anna University, Madras-600 025, India

*Department of Nuclear Physics, University of Madras, Madras-600 025, India

Abstract : A review of the high pressure studies made by the authors on the recent high T_c superconducting oxide materials has been presented. Both high pressure electrical resistivity and high pressure X-ray diffraction studies have been carried out on $La_{2-x}A_xCuO_4$ (where $A = Sr, Ba$) $RBa_2Cu_{3-x}M_xO_{7-y}$ ($R = Y, Gd, Dy, Ho$ and $Pr, M = Fe$) and $La_{1+x}Ba_{2-x}Cu_3O_{7-y}$ oxides at room temperature. A brief description of the experimental set up employed has also been presented.

Keywords : High T_c superconductors, high pressure, X-ray diffraction, electrical resistivity, structural transition.

PACS Nos : 74.70. Vy, 62.50. + p

1. Introduction

The importance of high pressure investigation was realised soon after the discovery of superconductivity around 30 K in a La-Ba-Cu-O system by Bednorz and Muller (1986). The superconducting transition temperature (T_c) of this system is increased by about 10 K under pressure of 15 kbar which is not observed in any known superconductors (Chu *et al* 1987). In fact this led to the successful idea of replacing La by the smaller Y, resulting to $YBa_2Cu_3O_7$ superconductor with a T_c of 90 K (Wu *et al* 1987). More than hundred papers were so far appeared on the effect of pressure on the high temperature (HT_c) superconductors (Wijngaarden and Griessen 1989). Present paper is a review of the work carried out in this laboratory for the past three years. It includes both high pressure electrical resistivity and high pressure X-ray diffraction studies carried out on HT_c superconductors at room temperature. A brief description of the experimental set up employed was also presented for the sake of completeness.

2. Experimental

2.1. Experimental set up for electrical resistivity measurements at high pressures :

The opposed anvil high pressure device is widely used in solid state studies, as this method is simple and easy to assemble compared to the other apparatus. For the present study also,

© 1992 IACS

this method has been chosen and fabricated. Figure 1(A) shows the schematic diagram of the experimental set up for electrical resistivity measurements at high pressures. The anvils have been made of EN 24 (AISI 4340) alloy steel, hardened to RC 60. The working face of the anvil is 10 mm and the outer diameter is 99 mm. As the taper angle decreases, the massive support factor increases and so the taper angle is chosen as 10 degrees so as to have maximum massive support. The load is applied through a 100 ton hydraulic press (Lawrence & Mayo (India) Pvt Ltd) and the sample cell assembly is placed in between the two opposed anvils.

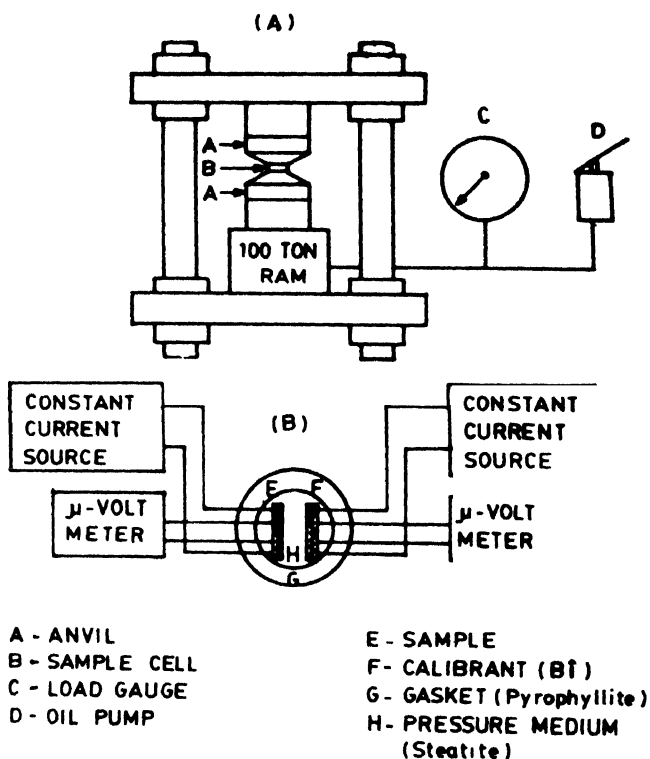


Figure 1. (A) The experimental set up for high pressure resistivity measurements. (B) Schematic diagram of the sample cell.

2.2. Sample cell assembly for resistivity study :

The sample cell assembly is schematically shown in Figure 1(B). The gasket is the pyrophyllite, and has the dimensions of 10 mm outer diameter, 2 mm inner diameter and a thickness of 0.5 mm. Steatite disk serves as the pressure transmitting medium. Simultaneous pressure calibration has been done by using metallic bismuth. The four probe method is used to measure the resistivity as most of the materials have low resistivity at room temperature. Tungsten wire of diameter 0.1 mm have been used as the electrical leads. They emerge from the cell via grooves between a pair of gaskets in the split gasket

configuration. High sensitivity digital microvoltmeter (Aplab 1041 DC Standard) and constant DC current source (Pacific Electronics Type PMV 16) have been used to measure the resistivity (ρ).

It is found that the alloy steel with nominal strength of 10 kbar can be used as the anvils upto 100 kbar for many cycles at room temperature. By controlling the dimensions of the gasket, it is possible to get good reproducibility in the pressure calibration.

2.3. Experimental set up for high pressure X-ray diffraction :

The measurements of unit cell parameters and the cell volume as a function of pressure can be done in a number of ways. Bridgman used the piston displacement measurements extensively upto 100 kbar (Bridgman 1971). X-ray diffraction studies offer the advantage of measuring the lattice parameters and studying the changes in crystal symmetry directly under pressure. In the last few years various types of high pressure X-ray apparatus have been developed (Bassett and Takahashi 1974, Graham 1986).

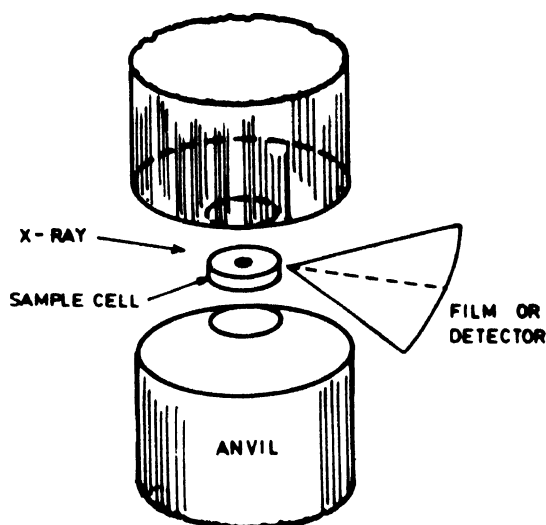


Figure 2. Schematic diagram of X-ray diffraction set up at high pressure.

In the present study, Bridgman opposed anvil principle has been used to obtain high pressure X-ray diffractogram. The basic principle is as shown in Figure 2. The X-ray beam is passed perpendicular to the axis of the load in the opposed anvils and the diffracted beam is detected either by film or X-ray detectors. For the present work a Bridgman anvil clamp type high pressure cell has been designed and developed. The clamp cell offers the advantage of loading and locking the high pressure at the hydraulic press itself, so that only the cell is placed near the X-ray generator.

2.4. Sample cell for X-ray diffraction study :

The sample cell is the heart of the high pressure cell. Amorphous boron wafer and amorphous boron with epoxy resin (40 wt. %) are used as the gasket. The dimensions of the sample cell are : the outer diameter is 3 mm, inner diameter 0.2–0.3 mm and thickness 0.3 mm. At the maximum pressure the gasket thickness reduces to 0.2 mm. The sample is mixed with NaCl and filled in the hole of the gasket. NaCl acts both as the internal calibrant and also as a pressure transmitting medium. The maximum pressure attained in this cell is about 80 kbar. Mo K_{α} radiation ($\lambda = 0.7107\text{\AA}$) from a rotating anode X-ray generator (Rigaku, Japan) of 12 kW power (60 kV, 200 mA), is employed. The target rotation is 6000 rpm and the beam focus size is 0.2×2 mm.

2.5. Proportional counter X-ray detecting system :

The diffraction patterns from the clamp cell are recorded by using the proportional counter detecting system (Victor Jaya and Natarajan 1988) and the details are given below. The detector is the krypton filled proportional counter and is scanned at a speed of 1.6 deg./min.

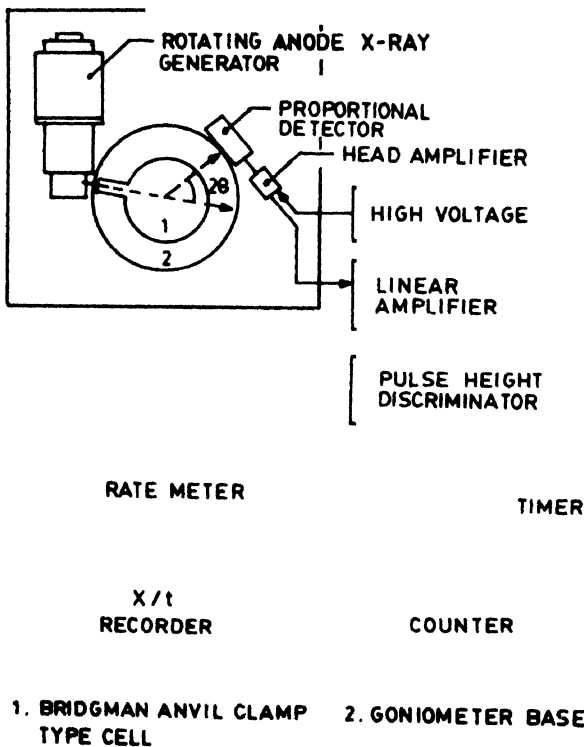


Figure 3. Block diagram of the high pressure X-ray diffractometer.

by using a synchronous motor. Fixed sample and moving detector technique is used. This low rate of scan gives better intensity data collection. Figure 3 shows the block diagram of

the diffractometer set up developed for the present high pressure X-ray diffraction work. Zirconium foil is used as the filter and it is placed at the detector window. This method was found to give better counts when the patterns are recorded at high pressures. The distance between the detector and the sample is 100 mm. The accuracy in 20 measurements is 0.08 degrees. The electronic parts used are manufactured by ECIL, India. The strip chart recorder (Ominiscribe 5000, of Digital Electronics Ltd, Bombay), is used to record the diffractograms.

2.6. Materials preparation and characterisation :

The compounds are synthesised by high temperature solid state reaction method using high purity oxides and carbonates. The samples are characterised by X-ray powder diffraction method (XRD) and superconductivity above 77 K was checked by Meissner effect. The high pressure X-ray diffraction and electrical resistivity measurements were carried out at room temperature upto 100 kbar.

3. Results and discussion

Most of the high pressure studies on oxide superconductors reported in the literature were related to the variation of T_c with pressure and some of them were carried out on multiphase samples especially of the Bi and Tl based superconductors. Further as the HT_c superconductors are very sensitive to its oxygen stoichiometry, substitution and its concentration and also on the processing condition, there is no systematic high pressure study in this regard. Results were often reported using a single technique only on a single composition. We have carried out high pressure study of a series of oxides of the LBCO (40 K superconductors) system and also of the YBCO (90 K superconductors) system. These systems were chosen as they were easy to prepare in single phase and also exhibit interesting behaviour with respect to the above parameters. We have always employed both resistivity study to monitor any variation in the electronic behaviour and also X-ray diffraction method to check actually the decrease of the unit cell volume and also any structural transition under pressure. The results are presented below together with the relevance of the system chosen for high pressure study.

3.1. 40K superconductors :

The superconducting oxides of the 214 family viz $La_{2-x}M_xCuO_4$ where $M = Ba, Sr, \text{ and } Ca$ show large increase of T_c under pressure which is about an order of magnitude larger than the previously studied superconductors (Chu *et al* 1987). These unusual large pressure effects are not clearly understood at present. In addition they also reveal anomaly in dT_c/dp leading to two pressure regions such that for $p < p_c$, $dT_c/dp = 0.1$ K/kbar while for $p > p_c$, $dT_c/dp = 0.04$ K/kbar, with $P_c = 6.4$ kbar for example in $La_{1.7}Ba_{0.3}CuO_4$ (Moret *et al* 1988).

The substitution of bismuth for lanthanum in the $\text{La}_{2-x}\text{Sr}_x\text{CuO}_4$ superconductors also increases the T_c as high as 42 K (Michel *et al* 1987). Bi ion is indeed characterized by the presence of the lone pair of electrons and can play the role of an anion, thereby can modify the oxygen framework. Also owing to its ability to form lamellar oxides including the recently discovered bismuth based superconductors, bismuth substitution in lanthanum compounds is worthwhile to examine.

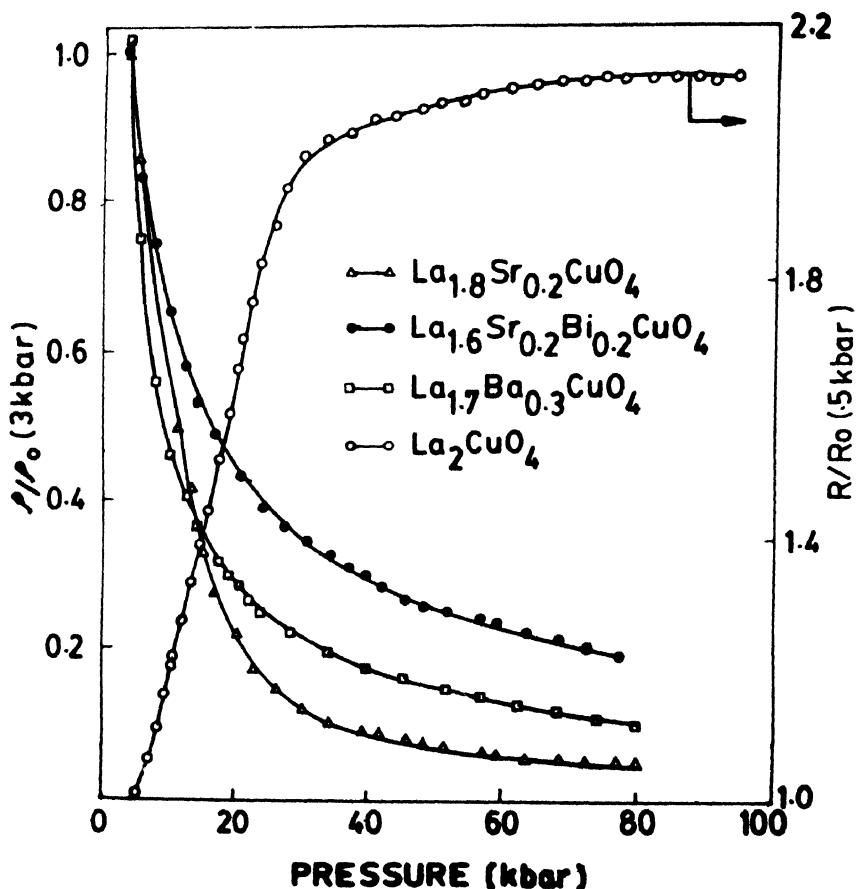


Figure 4. The variation of resistivity with pressure of $\text{La}_{1.8}\text{Sr}_{0.2}\text{CuO}_4$ (Δ), $\text{La}_{1.7}\text{Ba}_{0.3}\text{CuO}_4$ (\square) $\text{La}_{1.6}\text{Sr}_{0.2}\text{Bi}_{0.2}\text{CuO}_4$ (\bullet) and La_2CuO_4 (\circ) oxides at 300 K.

The variation of resistivity with pressure of $\text{La}_{1.8}\text{Sr}_{0.2}\text{CuO}_4$, $\text{La}_{1.7}\text{Ba}_{0.3}\text{CuO}_4$ and $\text{La}_{1.6}\text{Sr}_{0.2}\text{Bi}_{0.2}\text{CuO}_4$ are shown in Figure 4. For comparison, pressure variation of La_2CuO_4 is also in the same figure. The ' ρ ' of undoped oxide increases steeply with pressure up to 30 kbar and then remains nearly constant up to 80 kbar. This behaviour is typical of a semiconductor. However all the substituted oxides show sharp drop in ' ρ ' up to 30 kbar, indicating metallic behaviour. The ρ of $\text{La}_{1.8}\text{Sr}_{0.2}\text{CuO}_4$, which is a superconductor at 40 K, reaches a very low value compared to other oxides at 80 kbar.

The variation of unit cell volume (V) with pressure for La_2CuO_4 , $\text{La}_{1.8}\text{Sr}_{0.2}\text{CuO}_4$ and $\text{La}_{1.6}\text{Sr}_{0.2}\text{Bi}_{0.2}\text{CuO}_4$ oxides, as determined by X-ray powder diffraction method is shown in Figure 5. The ' V ' of La_2CuO_4 decreases continuously with pressure up to 70 kbar, but ' V ' of $\text{La}_{1.6}\text{Sr}_{0.2}\text{Bi}_{0.2}\text{CuO}_4$ decreases only to about 5% at this pressure. This can be due to Bi substitution which is known to improve the grain boundary cohesion of conventional ceramics. The compressibility values determined agrees well with the reported values (Dietrich *et al* 1987a, 1987b, Takahashi *et al* 1987). The ' d ' values of the observed peaks of

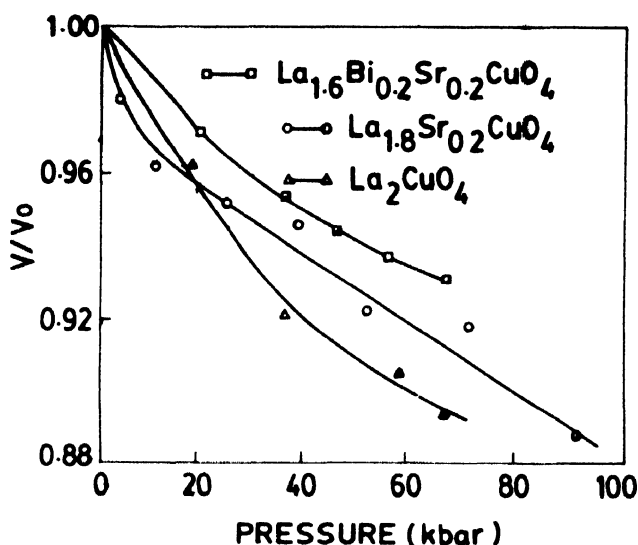


Figure 5. Reduced unit cell volume (V/V_0) vs pressure for $\text{La}_{1.8}\text{Sr}_{0.2}\text{CuO}_4$ (O), $\text{La}_{1.6}\text{Sr}_{0.2}\text{Bi}_{0.2}\text{CuO}_4$ (□) and La_2CuO_4 (Δ).

$\text{La}_{1.7}\text{Ba}_{0.3}\text{CuO}_4$ as a function of pressure is shown in Figure 6 and these values above 10 kbar could not be best fitted to the normal tetragonal structure. This may be due to a possible structural transition around 10 kbar as reported by Moret *et al* (1988).

3.2. 90 K superconductors :

The salient feature of $\text{YBa}_2\text{Cu}_3\text{O}_{7-x}$ superconductors is its sensitivity to oxygen stoichiometry. The orthorhombic structure of the superconductor with $x < 0.5$ results from the oxygen vacancy ordering and for $x > 0.5$ it undergoes structural transition to tetragonal, non-superconducting phase (Jorgenson *et al* 1987). This reversible orthorhombic to tetragonal transition also occurs on heating at 1023 K and thus the tetragonal phase can be easily realized by air annealing from this temperature (Schuller *et al* 1987). Application of high pressure can also cause the structural transition of the superconductors (Victor Jaya *et al* 1988). Further high pressure study of the tetragonal phase will also be interesting to check the possible transformation to other phases which may have still higher T_c .

Figure 7 shows variation of ' ρ ' with pressure for both the superconducting and non-superconducting phases of $\text{YBa}_2\text{Cu}_3\text{O}_{7-x}$. As expected the superconductor shows a sharp drop in ' ρ ', a typical of metals up to 20 kbar, while the tetragonal phase shows a relatively slow decrease of ' ρ ' extending up to 30 kbar pressure. At higher pressure, above 70 kbar, only the ' ρ ' of the superconductor starts increasing, indicating a transition around this pressure.

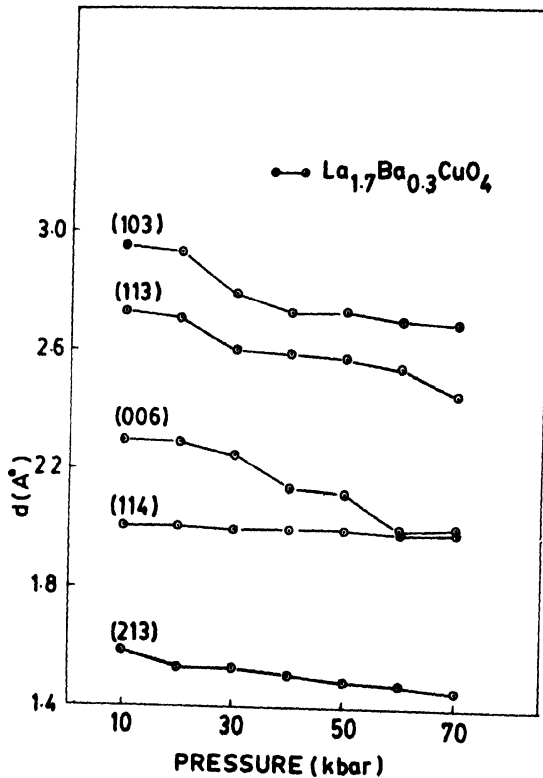


Figure 6. ' d ' values vs pressure for $\text{La}_{1.7}\text{Ba}_{0.3}\text{CuO}_4$.

The $\text{RBa}_2\text{Cu}_3\text{O}_{7-x}$ compounds with $R = \text{Nd}, \text{Sm}, \text{Gd}, \text{Dy}$ and Er also exhibit long range magnetic ordering at low temperatures, however the T_c is insensitive to the presence of these R ions. This result is in contrast to conventional superconductors where their presence of such impurities strongly suppress the T_c . The insensitivity of T_c to R ions indicates very weak exchange interaction between the R^+ magnetic moments and the superconducting electron spins. Application of high pressure can possibly influence this interaction. Olsen *et al* (1988) have carried out high pressure studies of $\text{RBa}_2\text{Cu}_3\text{O}_{7-x}$ with $R = \text{Y}$ and Eu and have reported orthorhombic to tetragonal transition at around 200 kbar. $\text{GdBa}_2\text{Cu}_3\text{O}_{7-x}$

under pressure remains orthorhombic with preferential decrease of c-axis up to 150 kbar as shown by Ecke *et al* (1988). The $\text{PrBa}_2\text{Cu}_3\text{O}_{7-x}$ although forms with the same crystal structure as the 123 phase, it is not superconducting and the lack of superconductivity in the Pr compound seems to be of structural origin, since the large Pr ion can possibly occupy

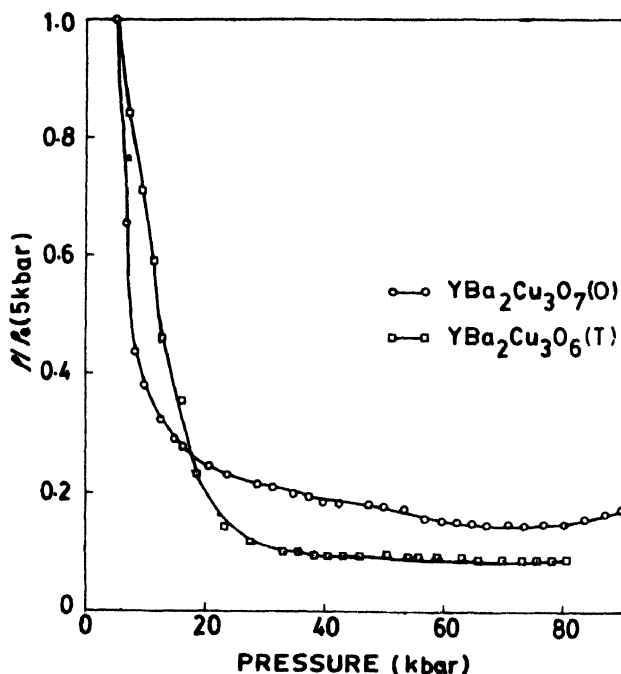


Figure 7. Normalised resistivity vs pressure of $\text{YBa}_2\text{Cu}_3\text{O}_7$ for Ortho (O) and Tetra (T) phases.

Ba position, leading to a strongly deformed coordination polyhedron (Dalichaouch *et al* 1988). This might affect T_c as the presence of the magnetic atom is adjacent to Cu-O chains. Pr in a mixed valence state in these compounds have been observed experimentally and Pr ion could in principle also substitute a Cu position. Metal Pr shows several structural modifications under pressure including an electronic transition (Wittig 1981). In this context high pressure studies of $\text{PrBa}_2\text{Cu}_3\text{O}_{7-x}$ will be very informative.

The variation of resistivity of $\text{RBa}_2\text{Cu}_3\text{O}_{7-x}$ (where R = Dy, Ho, Gd and Pr) oxides with pressure is shown in figure 8. Surprisingly all the oxides including the nonsuperconductor $\text{PrBa}_2\text{Cu}_3\text{O}_7$ shows a sharp drop in ' ρ ' up to 20 kbar pressure. Above 20 kbar all the superconductors show further decrease in ' ρ ' up to 80 kbar, but the resistivity of Pr compound starts increasing from 40 kbar onwards which may be due to some structural transition at this pressure.

Figure 9 shows the variation of the unit cell volume of the superconductors $\text{YBa}_2\text{Cu}_3\text{O}_7$, $\text{DyBa}_2\text{Cu}_3\text{O}_7$ and $\text{HoBa}_2\text{Cu}_3\text{O}_7$ and also of the nonsuperconducting $\text{YBa}_2\text{Cu}_3\text{O}_{7-x}$. Compressibility of the superconductor obtained from the above data, are in agreement with the reported values (Dietrich *et al* 1987a, 1987b). However the compressibility of the nonsuperconductor is low compared with those of superconductors. This is anticipated as the tetragonal phase is at less oxygen content than the superconductors.

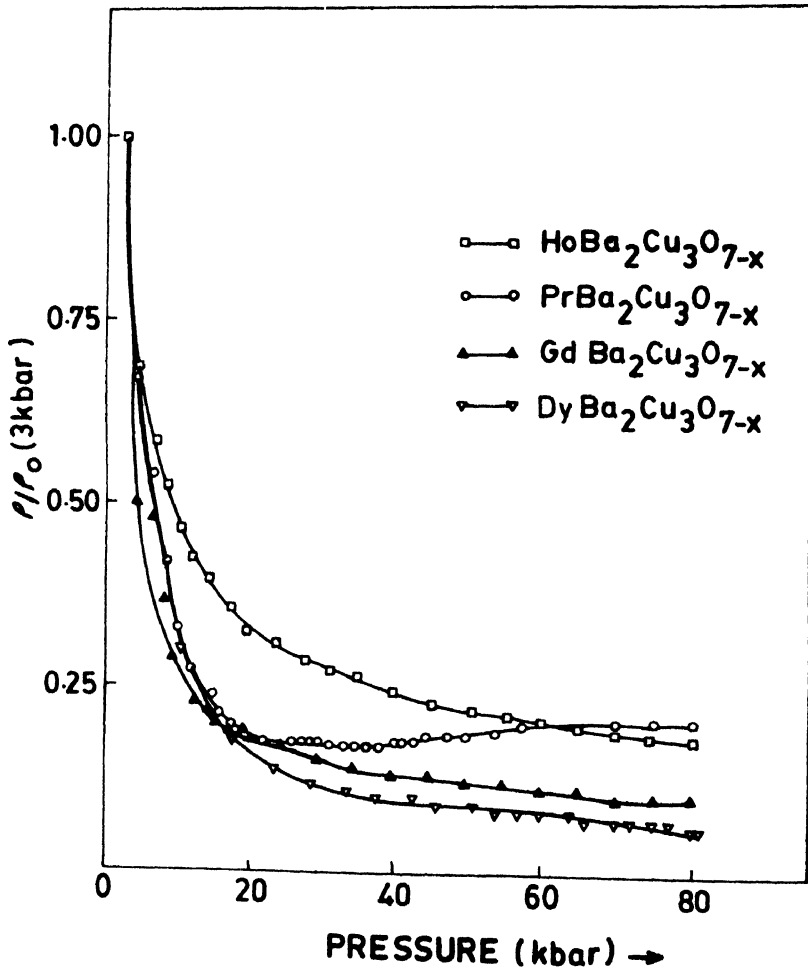


Figure 8. Normalised resistivity vs pressure for $\text{R}\text{Ba}_2\text{Cu}_3\text{O}_7$ (where R = Dy, Ho, Gd and Pr).

Partial substitution of Fe for Cu in the superconductor $\text{YBa}_2\text{Cu}_3\text{O}_7$ shows structural transition from orthorhombic to tetragonal phase (Maeno *et al* 1987). But the T_c is not sensitive to the transition although the magnetic atoms like Fe are distributed in the

superconducting plane rather than in any other sub lattice leading to interesting coexistence of magnetic ordering and superconductivity. For $X = 0.033$, it is possible to stabilize either T or O structures at room temperature by simply varying the final high temperature treatment in different atmospheres (Kurisu *et al* 1988). Air cooled sample is orthorhombic and superconducting above 77K while oxygen annealed sample is tetragonal and is not superconducting. Application of high pressure can induce superconductivity in the latter phase.

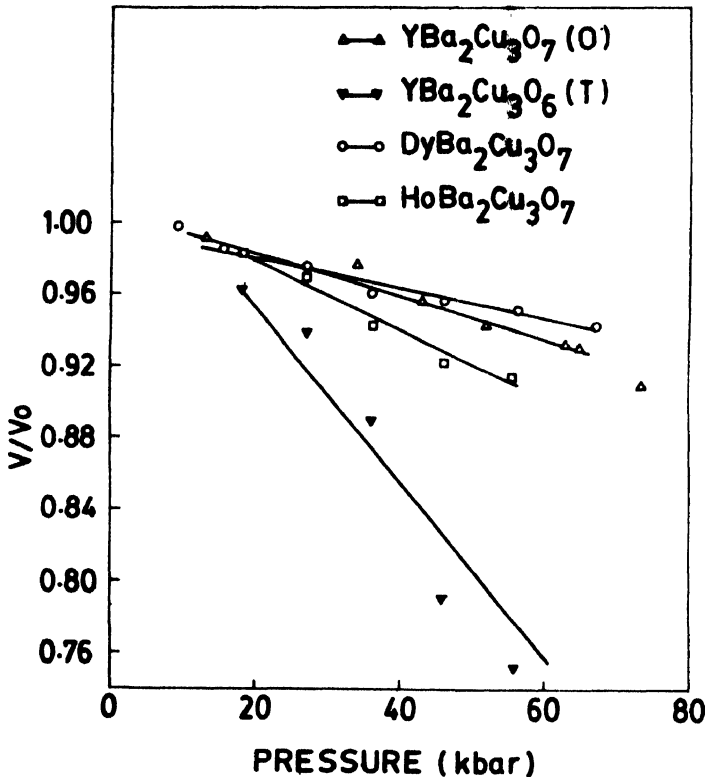


Figure 9. Reduced unit cell volume (V/V_0) vs pressure for $\text{RBa}_2\text{Cu}_3\text{O}_7$ (where $R = \text{Dy}, \text{Ho}, \text{Y(O)}$ and (T)).

Figure 10 shows the ' ρ ' variation with pressure of $\text{YBa}_2\text{Cu}_{2.91}\text{Fe}_{0.09}\text{O}_{7-x}$ oxygen annealed sample. For comparison the ' ρ ' behaviour of the air annealed superconducting sample of the same composition is also shown in the same figure, which is same as that of any other ceramic superconductors studied earlier. However, ' ρ ' of the nonsuperconducting phase initially increases up to 15 kbar followed by a continuous decrease up to 80 kbar similar to that of the air cooled superconducting phase. As the initial increase of ' ρ ' with pressure is typical of semiconductors, the observed behaviour at 15 kbar suggests possible metallization around this pressure.

3.3. $La_{1+x}Ba_{2+x}Cu_3O_{7+y}$ system :

The system mentioned above, depending upon the value of x , leads to three different compounds. viz $La_3Ba_3Cu_6O_{14.1}$, $La_4BaCu_5O_{13.4}$ and $La_{1.15}Ba_{1.85}Cu_3O_7$. $La_3Ba_3Cu_6O_{14.1}$ being semiconductor shows a slow decrease under pressure in its normalized resistivity value up to 80 kbar (Figure 11). $La_4BaCu_5O_{13.4}$ which is metallic, exhibits a steeper fall up to 11 kbar, a slow decrease up to 50 kbar and almost constant value up to 80 kbar as a function of

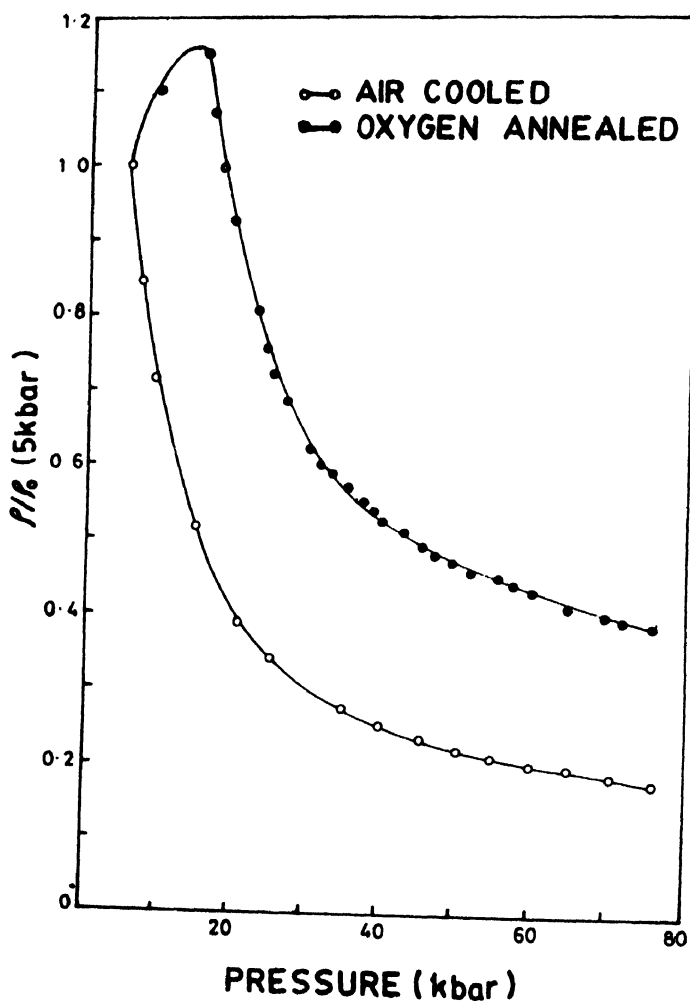


Figure 10. Normalised resistivity vs pressure for $YBa_2Cu_{2.19}Fe_{0.09}O_{7-y}$ air cooled (O) and oxygen annealed (•) oxides.

pressure (Figure 11). Superconducting $La_{1.15}Ba_{1.85}Cu_3O_7$, behaves in a different manner. Its normalized resistivity curve falls steep up to 9 kbar, decreases gradually up to 50 kbar and

shows constant level almost coinciding with the value of normalized resistivity of $\text{La}_3\text{Ba}_3\text{Cu}_6\text{O}_{14.1}$.

The structure of the superconductor as confirmed by X-ray powder diffraction method is orthorhombic while that of the other oxides are tetragonal. The variation of normalised unit cell volume with pressure of all the oxides is shown in Figure 12. It is evident from the figure that the compressibility of the superconductor is the highest while that of the metallic oxide is the lowest of all the three.

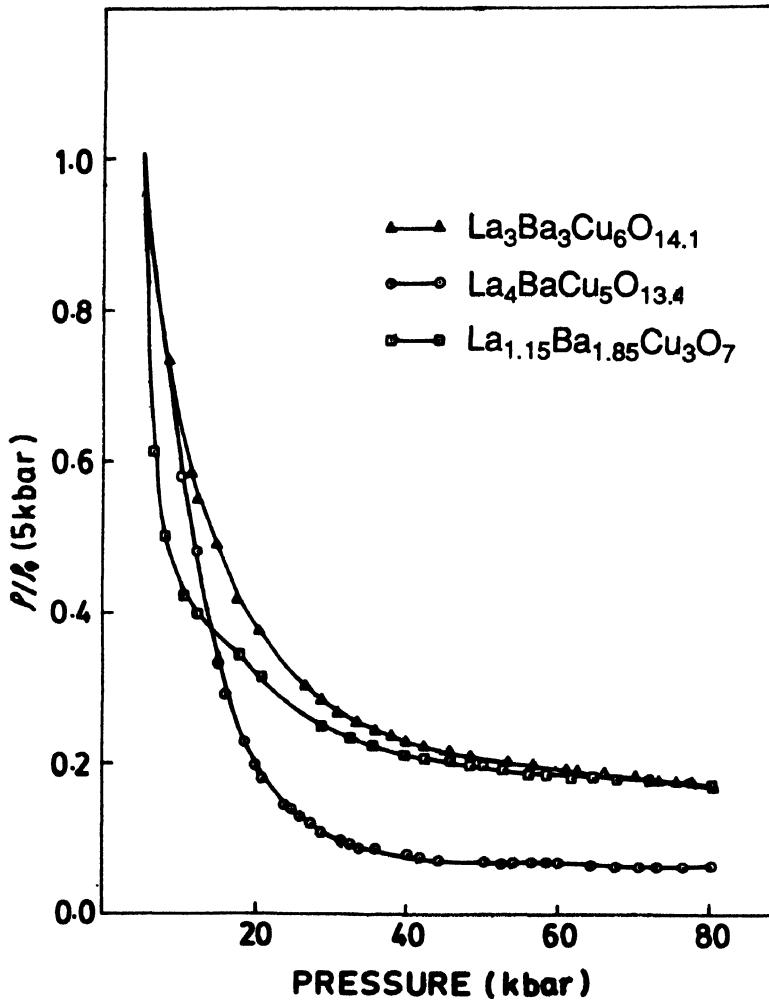


Figure 11. Normalised resistivity of $\text{La}_3\text{Ba}_3\text{Cu}_6\text{O}_{14.1}$ (Δ), $\text{La}_4\text{BaCu}_5\text{O}_{13.4}$ (O) and $\text{La}_{1.15}\text{Ba}_{1.85}\text{Cu}_3\text{O}_7$ (\square) oxides under pressure.

A summary of the high pressure resistivity and high pressure X-ray diffraction results of the high T_c superconductors studied are given in Table 1.

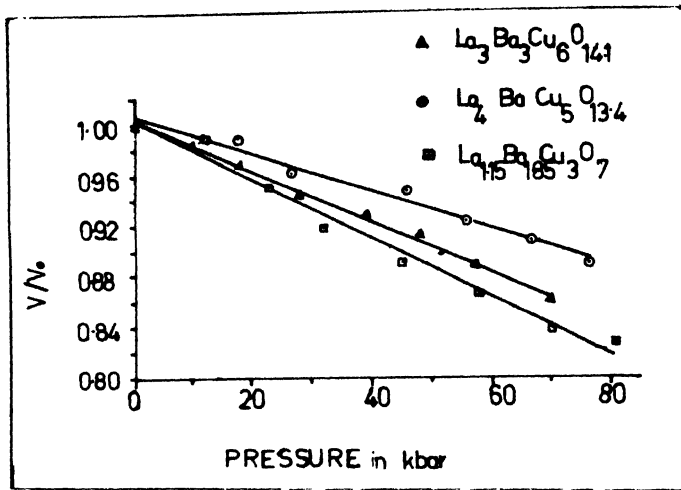


Figure 12. The variation of normalized unit cell volume with pressure of all the oxides.

Table 1. Cell parameters, resistivity and compressibility data.

Samples	Cell parameters			ρ (5 kbar)	Compressibility
	$a(\text{Å})$	$b(\text{Å})$	$c(\text{Å})$	$\Omega\text{-cm}$	(kbar^{-1})
$\text{La}_{1.8}\text{Sr}_{0.2}\text{CuO}_4$	3.76(2)	3.76(2)	13.13(5)	—	—
$\text{La}_{1.6}\text{Sr}_{0.2}\text{Bi}_{0.2}\text{CuO}_4$	3.75(6)	3.75(6)	13.19(20)	1.29×10^{-2}	6.45×10^{-4}
$\text{La}_{1.7}\text{Ba}_{0.3}\text{CuO}_4$	3.75(5)	3.75(5)	13.32(2)	9.78×10^{-2}	—
$\text{YBa}_2\text{Cu}_3\text{O}_{7-x}$ (O)	3.82(8)	3.89(8)	11.62(4)	1.45×10^{-3}	10.5×10^{-4}
$\text{YBa}_2\text{Cu}_3\text{O}_{7-x}$ (T)	3.86(1)	3.86(1)	11.63(4)	7.85×10^{-1}	4.73×10^{-3}
$\text{HoBa}_2\text{Cu}_3\text{O}_{7-x}$	3.84(5)	3.89(7)	11.68(2)	5.31×10^{-2}	1.15×10^{-3}
$\text{PrBa}_2\text{Cu}_3\text{O}_{7-x}$	3.92(5)	3.92(5)	11.76(2)	7.53×10^{-2}	5.59×10^{-3}
$\text{GdBa}_2\text{Cu}_3\text{O}_{7-x}$	3.83(3)	3.89(5)	11.67(7)	7.92×10^{-2}	1.25×10^{-3}
$\text{DyBa}_2\text{Cu}_3\text{O}_{7-x}$	3.83(6)	3.84(6)	11.89(20)	1.69×10^{-2}	7.69×10^{-4}
$\text{La}_3\text{Ba}_3\text{Cu}_6\text{O}_{14.1}$	5.52(5)	5.52(5)	11.89(13)	9.14×10^{-1}	1.98×10^{-3}
$\text{La}_4\text{BaCu}_5\text{O}_{13.6}$	8.53(7)	8.53(7)	3.87(4)	1.45×10^{-3}	1.49×10^{-3}
$\text{La}_{1.15}\text{Ba}_{1.85}\text{Cu}_3\text{O}_7$	3.67(0)	3.99(1)	11.63(3)	1.65×10^{-2}	2.30×10^{-3}

Acknowledgments

Thanks are due to UGC for funding the research project. Prof GV Subba Rao, Prof R Srinivasan and their colleagues at the Indian Institute of Technology, Madras are acknowledged with thanks for their support in numerous ways to carry out the research

work. Thanks are due to Dr K Govindarajan and his colleagues at IGCAR, Kalpakkam for their help in high pressure instrumentation.

References

- Bassett W A and Takahashi T 1974 *Advances in High Pressure Research* Vol 4 ed. Wantrof J R (Academic : London) p 165
- Bednorz J G and Muller K A 1986 *Z Phys* **64** 189
- Bridgman P W 1971 *Proc. Am Acad. Art. Sci.* **42** 3239
- Chu C W, Hor P H, Meng R L, Gao L, Huang Z J and Wang Y Q 1987 *Phys. Rev. Lett.* **58** 405
- Dalichaouch Y, Torikachvili M S, Early E A, Lee B W, Seaman C L, Yang K N, Zhou H and Maple M B 1988 *Solid. State. Commun.* **65** 1001
- Dietrich M R, Fietz W H, Ecke J and Politis C 1987a *Jpn. J. Appl. Phys.* **26** 1113
- Dietrich M R, Fietz W H, Ecke J, Obst B and Politis C 1987b *Z Phys.* **B66** 283
- Ecke J, Fietz W H, Dietrich M R, Wassilew C A, Wuhl H and Flukiger 1988 *Physica B+C* eds. J Muller and J S Olsen
- Graham E K 1986 *J Geo. Res* **91** 4630
- Jorgenson J D, Voal B W, Kwok W K, Crabtree C W, Unezawa A, Nowicki L J and Paulikas A P 1987 *Phys Rev* **B36** 5731
- Kursu M, Kumagai K, Maeno Y and Fugita T 1988 *Physica C* **152** 339
- Maeno Y, Kato M, Aoki Y and Fugita T 1987 *J Appl. Phys* **26** L1982
- Michel C, Prevast J, Deslandes F, Raveau, Beille J, Carbanal R, Lejay P, Sulpice A and Tholenie J L 1987 *Z Phys.* **B68** 417
- Moret R, Goldman A I and Moodenbaugh A 1988 *Phys Rev.* **B37** 7867
- Olsen J S, Steenstrup S, Johannsen I and Gerward L 1988 *Z. Phys.* **B72** 165
- Schuller I K, Hinks D G, Beno M A, Capone II D W, Soderholm L, Locquet J P, Bruynseraede Y, Segre C U and Zhang K 1987 *Solid State Commun* **63** 385
- Takahashi H, Murayama S, Yoma S, Mori N, Ustumi W and Yagi T 1987 *Jpn. J Appl Phys.* **26** 1109
- Victor Jaya N and Natarajan A 1988 *Rev. Sci. Instrum.* **59** 510
- Victor Jaya N, Natarajan S, Natarajan S and Subba Rao GV 1988 *Solid State Commun.* **67** 51
- Wijnngaarden J Rinke and Gnessen R 1989 *Studies of the High Temperature Superconductors* Vol 2 ed. A V Narlikar (New York : Nova Science) p 29
- Wittig J 1981 *Physics of Solids Under Pressure* p 283
- Wu M K, Ashburn J R, Tomg C J, Hor P H, Meng R L, Gao L, Huang Z J, Wang Y Q and Chu C W 1987 *Phys. Rev. Lett.* **58** 908